Chinese Chemical Letters 36 (2025) 110618

Contents lists available at ScienceDirect

Chinese Chemical Letters

journal homepage: www.elsevier.com/locate/cclet

Review on near-infrared absorbing/emissive carbon dots: From preparation to multi-functional application

Yupeng Liu[a], Hui Wang[b,c], Songnan Qu[a,*]

[a] Joint Key Laboratory of Ministry of Education, Institute of Applied Physics and Materials Engineering (IAPME), University of Macau, Macau SAR 999067, China
[b] University of Science and Technology of China, Hefei 230026, China
[c] High Magnetic Field Laboratory, Hefei Institutes of Physical Science, Chinese Academy of Science, Hefei 230031, China

ARTICLE INFO

Article history:
Received 30 August 2024
Revised 4 November 2024
Accepted 6 November 2024
Available online 7 November 2024

Keywords:
Carbon dots
Near-infrared
Luminescence
Photothermal therapy
Photodynamic therapy
Afterglow
Laser

ABSTRACT

Carbon dots (CDs) are an emerging class of zero-dimensional carbon nano optical materials that are as promising candidates for various applications. Through the exploration of scientific researchers, the optical band gap of CDs has been continuously regulated and red-shifted from the initial blue-violet light to longer wavelengths. In recent years, CDs with near-infrared (NIR) absorption/emission have been gradually reported. Because NIR light has deeper penetration and lower scattering and is invisible to the human eye, it has great application prospects in the fields of biological imaging and treatment, information encryption, optical communications, *etc.* Although there are a few reviews on deep red to NIR CDs, they only focus on the single biomedical direction. There is still a lack of comprehensive reviews focusing on NIR (≥700 nm) absorption and luminescent CDs and their multifunctional applications. Based on our research group's findings on NIR CDs, this review summarizes recent advancements in their preparation strategies and applications, points out the current shortcomings and challenges, and anticipates future development trajectories.

1. Introduction

When an incident beam irradiates biological tissue, a portion is reflected while the rest enters the tissue. This penetrating light scatters within the tissue, with some reaching deep enough to activate fluorescent materials, generating a fluorescence signal. As this fluorescence travels back toward the tissue surface, it also scatters. Simultaneously, the incident light, scattered light, and fluorescence interact with the tissue, leading to autofluorescence. Scattering diminishes the desired fluorescence signal, while autofluorescence elevates background noise, both hindering fluorescence imaging (FLI) (Fig. S1a in Supporting information). To enhance imaging quality, it is crucial to have light waves that deeply penetrate, scatter minimally, and induce low autofluorescence upon tissue interaction [1]. The near-infrared (NIR) light band (700–1700 nm) has such advantages as deeper penetration, lower scattering, and autofluorescence when compared with the visible band, which can be utilized in bioapplications (Figs. S1b-d in Supporting information) [2,3].

Up to now, NIR luminescent materials such as carbon nanotubes (CNTs) [4], inorganic semiconductor quantum dots (QDs) [5], and organic dyes [6,7] have been widely studied. However, these materials still have some shortcomings, such as the cumbersome synthesis steps of NIR organic dyes, high prices, and poor resistance to photobleaching. Inorganic semiconductor quantum dots bring potential biosafety, and environmental pollution risks due to the presence of precious metals. In contrast, carbon dots (CDs) materials, a novel type of emerging carbon nanomaterials following in the footsteps of fullerene, CNTs, and graphene [8], have just been developed in the past 10–20 years [9,10] and can overcome the above shortcomings. They can be classified into various types such as graphene quantum dots (GQDs), carbon nanodots (CNDs), carbon quantum dots (CQDs), and carbonized polymer dots (CPDs). This zero-dimensional carbon nanomaterial with a size of <10 nm requires only one or two steps of simple synthesis or modification following relatively easy purification [11]. The raw materials are widely available, almost from all carbon-containing substances, and are inexpensive. More importantly, the low cytotoxicity and good biocompatibility of CDs make them ideal as biological application reagents [12,13].

The synthesis methods of CDs generally include "top-down" and "bottom-up" methods [8,14]. The former involves strong acid strip-

* Corresponding author.
E-mail address: songnanqu@um.edu.mo (S. Qu).

https://doi.org/10.1016/j.cclet.2024.110618
1001-8417/

ping, laser ablation, or electrochemical etching of bulk carbon materials (such as coal, graphite, graphene). Due to the extreme reaction conditions and the small types of available raw bulk carbon materials, the CDs obtained by this method mostly emit light in the visible light band (blue-green light band) with a low photoluminescence quantum yield (PLQY). For example, in 2006, Sun *et al.* generated carbon nanoparticles by laser ablating a carbon target and obtained brightly fluorescent CDs (PLQY ~4%–10%) through surface passivation with polyethylene glycol (PEG) [9]. In 2010, Pan *et al.* obtained blue luminescent GQDs through hydrothermal cutting of graphene sheets [15]. The latter "bottom-up" method, as the name implies, utilizes small carbon-containing molecules as precursors to prepare CDs through hydrothermal method, solvothermal method, microwave-assisted synthesis method, solid-state pyrolysis method [16–19], and so on. Because of the controllability of the raw material types, reaction solvent types, reaction temperature, and time, it has become the mainstream method for boosting the fabrication of multicolor emissive CDs. For example, Jiang *et al.* synthesized green, blue, and red luminescent CDs for multicolor cell imaging using *o*-phenylenediamine, *m*-phenylenediamine, and *p*-phenylenediamine as single reactants *via* a hydrothermal method [20]. In 2017, by controlling the protonation of the reaction solvent, Qu's research group synthesized multi-color CDs with gradually increasing sizes using citric acid and urea as raw materials. These CDs were then used in the fabrication of white light-emitting diodes (WLEDs) [21].

With vigorous development in this field, the luminescence of CDs has evolved from the early blue-green luminescence to the current long-wavelength luminescent CDs (such as red and NIR emitting CDs), which are increasingly being reported [22]. However, the research on NIR CDs is still in its early stages (Fig. S2 in Supporting information), there are still blind spots in the luminescence mechanism and synthetic design of NIR CDs. Although there were some reported reviews about red to NIR CDs [23–26], they only focused on the biomedical applications of CDs. Based on this, this review mainly discusses CDs with absorption or luminescence bands no less than 700 nm and systematically introduces common preparation strategies and multi-functional application scenarios of NIR CDs (Fig. 1) [8,27–31]. Finally, the current challenges in this field and future development directions are also summarized and outlooked.

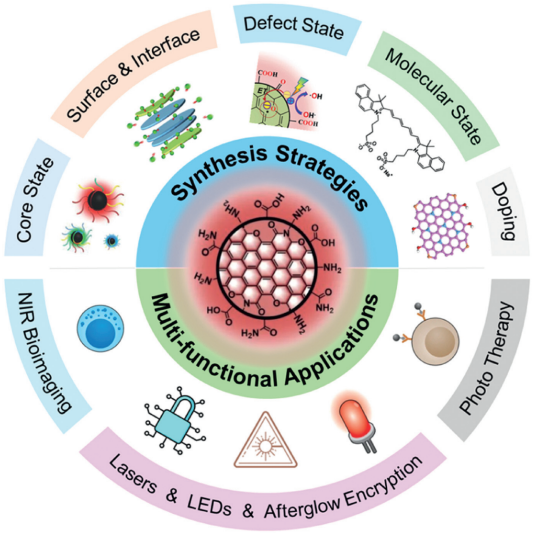

Fig. 1. Schematic diagram of the synthesis strategies and multi-functional applications of NIR CDs. Reproduced with permission [8,27–31]. Copyright 2022, Springer Nature; Copyright 2018, 2019 & 2023, John Wiley and Sons; Copyright 2020, Elsevier; Copyright 2022, The authors.

2. Synthesis strategy of NIR CDs

According to the corresponding luminescence mechanism, strategies for regulating NIR absorption/luminescence can be formulated. Current research reveals that the luminescence mechanism of CDs can be summarized as follows. The first is core-state luminescence [21]. By increasing the size of the conjugated domain of the carbon core, its luminescence band gap can be effectively narrowed, so that it produces NIR luminescence [31]. The second is surface and interface-state luminescence [32]. Electron-withdrawing groups can be artificially introduced on their surface to obtain NIR CDs. Another method is to form supra-CDs through the assembly of the surface and interface to achieve NIR luminescence. The third is molecular-state luminescence, which is the light emitted due to the covalent connection of the molecular fluorophore skeleton to the surface or core of the CDs [33]. It can be considered to use organic dyes or polymers with NIR luminescence as precursors to prepare NIR CDs. The fourth is defect-induced luminescence [29]. Constructing oxidation defects on the core of the CDs can effectively achieve defect-state NIR luminescence. In addition, the emission of CDs can be red shifted by element doping. The synergistic effect of element doping and other strategies is one of the effective methods for obtaining NIR CDs [27].

2.1. Enlargement of the conjugated domain

The redshift of the luminescence of CDs as their conjugated size increases has been supported by numerous literature reports and theoretical calculations (Fig. 2a) [21,27,34,35]. The choice of a protic/aprotic solvent can influence the extent of carbonization and conjugation of the carbon core during the formation of CDs [36]. Qu's group placed citric acid and urea in three solvents (water, glycerol, *N*,*N*-dimethylformamide) with gradually decreasing protonity for a hydrothermal/solvothermal reaction and obtained three types of CDs with gradually increasing sizes, their luminescence also shifted from blue to green and red (Fig. 2b) [21]. Xiong *et al.* utilized various organic solvents, both individually or in a mixture, and sulfuric acid aqueous solutions of different concentrations to control the dehydration and carbonization process of the precursor, achieve controllable growth of the size of the conjugated domain of CDs (Fig. 2c), and produce luminescent CDs of different sizes with red-shifted emission from blue light to NIR (745 nm) [27].

Theoretical calculations show that the optical band gap of conjugated CDs with a particle size of about 2 nm can reach the NIR band, while most of the CDs reported so far exceed this size, indicating that the size of CDs observed by transmission electron microscopy cannot fully reflect the size of the carbon core conjugated domain. CDs prepared from non-conjugated small molecule raw materials (such as citric acid and ethylenediamine) mostly emit light in the visible light region. However, using phenylenediamine with a benzene ring as a raw material, CDs from red to NIR light can be easily obtained. For example, Lu *et al.* utilized *o*-phenylenediamine and dopamine as raw materials to synthesize NIR luminescent CDs with an emission peak at 710 nm. Dopamine and *o*-phenylenediamine were chosen because their molecular structures result in larger conjugated sp^2 domains [37].

Furthermore, Qu's group proposed the idea of using molecules with larger conjugated domains as precursors to synthesize CDs with a higher conjugation degree. Raw materials with five benzene ring conjugated structures, such as perylene and its derivatives, have been utilized in the development of NIR luminescent CDs. They screened perylenetetracarboxylic dianhydride (PTCDA) with five benzene rings as conjugated raw materials and combined them with urea molecules under solvothermal conditions to produce CDs with a dominant NIR emission peak at 751 nm in water (Fig. 2d) [31].

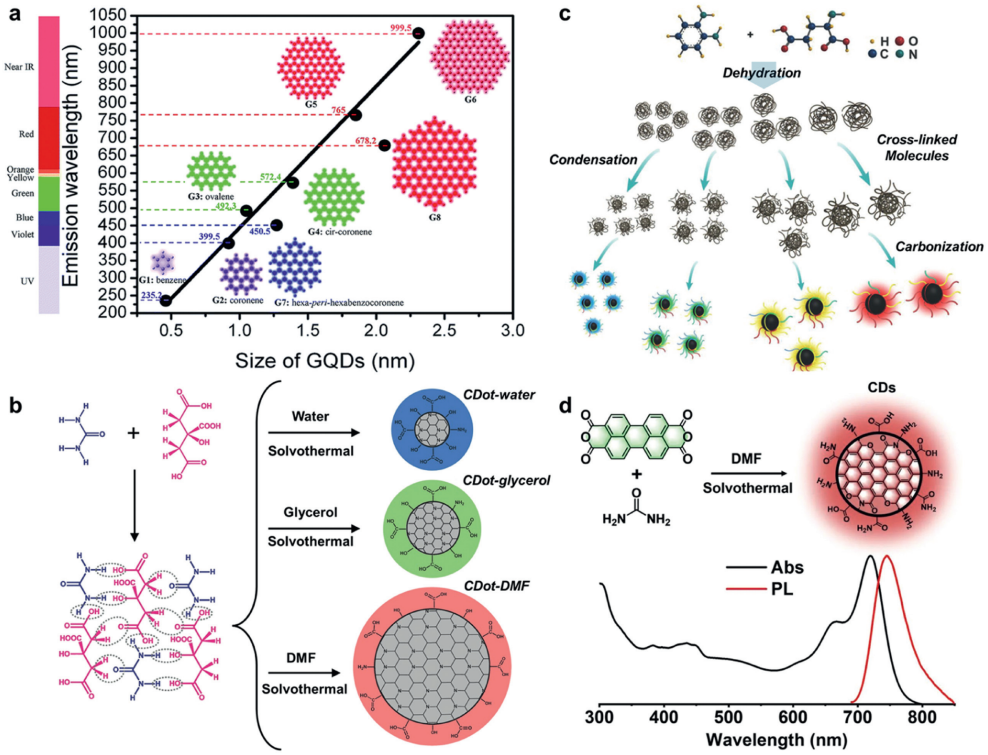

Fig. 2. (a) Theoretically calculated band gaps and emission peaks of GQDs with different diameters. Reproduced with permission [34]. Copyright 2014, Royal Society of Chemistry. (b) CDs of different sizes prepared in different solvents. Reproduced with permission [21]. Copyright 2017, John Wiley and Sons. (c) CDs of different sizes were obtained using *o*-phenylenediamine as a precursor under different solvent conditions. Reproduced with permission [27]. Copyright 2018, John Wiley and Sons. (d) NIR CDs obtained under solvothermal conditions using the large conjugated molecule PTCDA as a precursor. Reproduced with permission [31]. Copyright 2017, The authors.

2.2. Surface and interface engineering

2.2.1. Surface state regulation

The luminescence originating from the functional groups on the surface of CDs is called surface state luminescence. Modifying and regulating the surface state of CDs is one of the effective ways to narrow the band gap of CDs. Based on the orange-emitting CDs they prepared from the solvothermal reaction of citric acid and urea in DMF [38], Qu's group further modified the CDs with molecules or polymers rich in sulfoxide/carbonyl (S=O/C=O) groups (Fig. 3a), like dimethyl sulfoxide (DMSO). These electron-withdrawing groups (S=O/C=O) can interact with the outer layers and edges of CDs, inducing increased surface oxidation and causing the outer layers of CDs to bend. This surface treatment induces the appearance of NIR absorption bands (715–724 nm) and efficient NIR emission (750–760 nm) with PLQY up to 10% in these CDs [32].

2.2.2. Self-assembly and stripping

In 2016, Qu's group constructed supra-CDs with strong visible-NIR absorption bands centered at 700 nm by assembling UV-absorbing CDs with spatially separated surface energy levels [39]. In 2021, Qu's group utilized microwave-assisted exfoliation to separate multi-layer CDs into few-layer CDs. The NIR absorption peak has enhanced from the shoulder peak to the main peak [28]. The surface area of the exfoliated oligolayer CDs increases, and more electron-withdrawing groups are attached to the surface or edges, resulting in the main NIR absorption band reaching a peak at 724 nm and it also exhibits up-conversion NIR luminescence (Figs. 3b and c).

2.2.3. Hybridization and heterojunction

By mixing with other materials to form hybrid materials or heterojunctions, the NIR absorption or emission of CDs composites can be effectively enhanced. Geng *et al.* synthesized CDs from 1,3,6-trinitropyrene and branched polyethyleneimine (BPEI) by microwave-assisted hydrothermal method [40], and then compounded them with different materials to form hybrid materials. Utilizing a similar strategy, Geng and colleagues systematically studied the compounding of the above CDs with materials with high photothermal conversion efficiency (PCE) such as black phosphorus [41], TiCN nanosheet [42], Nb_2C nanosheet [43], WS_2 nanosheet (Fig. 3d) [30]. The absorption of these composites from visible light to NIR is significantly enhanced with high PCE for tumor PTT.

2.3. Defect state regulation

Defect-induced NIR luminescence has been widely reported in materials such as CNTs [44], metallic nanoclusters [45], and inorganic nanocrystals [46], but there are only a few reports in CDs [29].

Recently, Qu's group reported a simple method to induce oxygen-related defects in CDs through post-oxidation with 2-iodoxybenzoic acid. Some nitrogen atoms in CDs are replaced by oxygen atoms, and the unpaired electrons in these oxygen-related defects rearrange the electronic structure of oxidized CDs (ox-CDs), leading to the emergence of new NIR absorption bands at 720 nm and emission bands at 760 nm. These defects not only contribute to enhanced NIR bandgap emission but also serve as capture agents for photoexcited electrons, promoting efficient charge separation at the surface. This process generates hydroxyl radicals upon visible light irradiation. Utilizing the Janus optical properties of ox-CDs, we achieved *in vivo* NIR FLI of sentinel lymph nodes around tumors and effective photothermal-enhanced tumor photocatalytic therapy (PCT) [29].

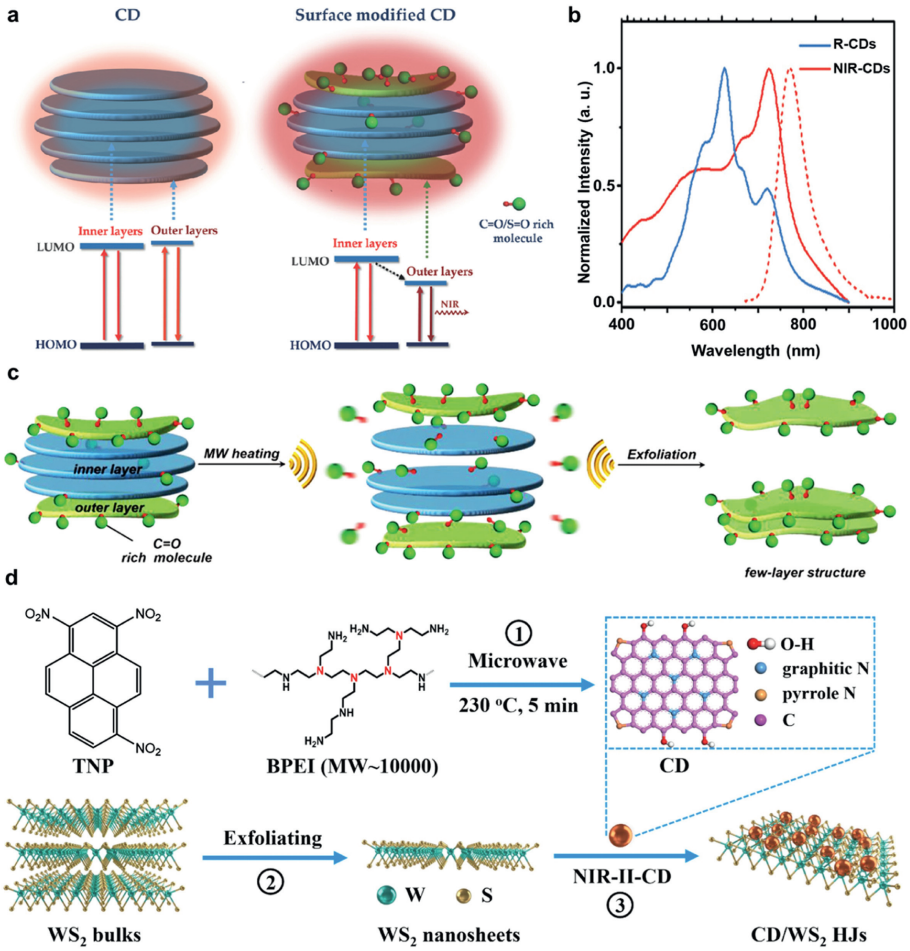

Fig. 3. (a) Schematic of structure and energy level alignments of nontreated CDs (left column) and CDs modified with S=O/C=O-rich molecules (right column). Reproduced with permission [32]. Copyright 2018, John Wiley and Sons. (b) Absorption spectra (solid lines) of R-CDs and NIR-CDs, and PL spectra of NIR-CDs (dashed line) in DMF. (c) Schematics of the formation process of NIR-CDs through the microwave (MW)-assisted exfoliation of R-CDs. Reproduced with permission [28]. Copyright 2019, John Wiley and Sons. (d) The preparation procedure of CD/WS_2 HJs. Reproduced with permission [30]. Copyright 2022, Elsevier.

2.4. Molecule state regulation

The principle of using the molecular luminescence mechanism of CDs to regulate their luminescence is to retain the optical properties of the raw material molecules. Usually, NIR dye molecules or polymers are used as precursors, and the CDs obtained by reacting them alone or with other raw materials will inherit their NIR optical properties. Among them, cyanine dyes are the most widely used [33,47–53]. Although the synthesis of cyanine (Cy) dyes is complex, and Cy dyes are expensive with poor water solubility, Cy dyes-derived CDs can inherit NIR absorption/emission properties. Additionally, they can exhibit enhanced photothermal conversion effects and increased anti-photobleaching ability.

As early as 2016, Xie *et al.* obtained water-soluble NIR CDs (CyCD) by hydrothermal reaction of hydrophobic Cy dye CyOH and water-soluble polyethylene glycol (PEG800) (Fig. 4a). Its emission peak is at 805 nm, the absorption peak is at 770 nm, and it inherits the photothermal properties of CyOH, with a PCE of 38.7% [33]. Fan *et al.* utilized cyanine dye Cy-COOH and Cy7-CH_3 as raw materials to synthesize NIR CDs with emission peaks at 710 nm [51] and 1160 nm [47], respectively. Jiang *et al.* used the cyanine dye indocyanine green (ICG) as the sole raw material to synthesize NIR CDs (ICG-CDs) with significantly improved photothermal efficiency [53]. Cyanine dyes have two indole structures on both sides and a methylene bridge in the middle. Zhu *et al.* imitated the structure of cyanine dyes, used aldehyde-containing conjugated CPDs as conjugated bridges, and covalently linked them with a group of indole derivatives through the Knoevenagel reaction to obtain a series of NIR CPDs, which emit light in the NIR I and NIR II regions (Fig. 4b) [54].

Polymers such as polythiophene and its derivatives can also be used as raw materials to produce NIR CDs [55–58]. For example, Ge *et al.* utilized single positively charged CDs as building blocks and negatively charged amphiphilic sodium dodecyl benzene sulfonate (SDBS) molecules as cross-linking agents to synthesize CDs through a straightforward non-covalent method based on cooperative charge interaction. The nanospheres (CDNS) exhibit a new NIR emission peak at 730 nm [58]. Zhang *et al.* utilized polythiophene quaternary ammonium salt derivatives (PT2) and diphenyl diselenide as raw materials to synthesize NIR CDs with emission peaks at 731 nm and 820 nm (Fig. 4c) [56].

2.5. Heteroatom doping

Heteroatom doping has proven to be a feasible strategy for narrowing the band gap of CDs. To obtain NIR absorbing/emitting CDs, metal elements such as Mn, Fe, Co, Ni, Cu, and rare earth elements are often used as dopants for CDs [50,59–62], and B, N, F, P, S, Se, *etc.* are often used as non-metallic element dopants [56,63–67].

2.5.1. Metal element doping

It has been widely reported that CDs have new NIR absorption peaks or emission peaks due to metal element doping [68,69].

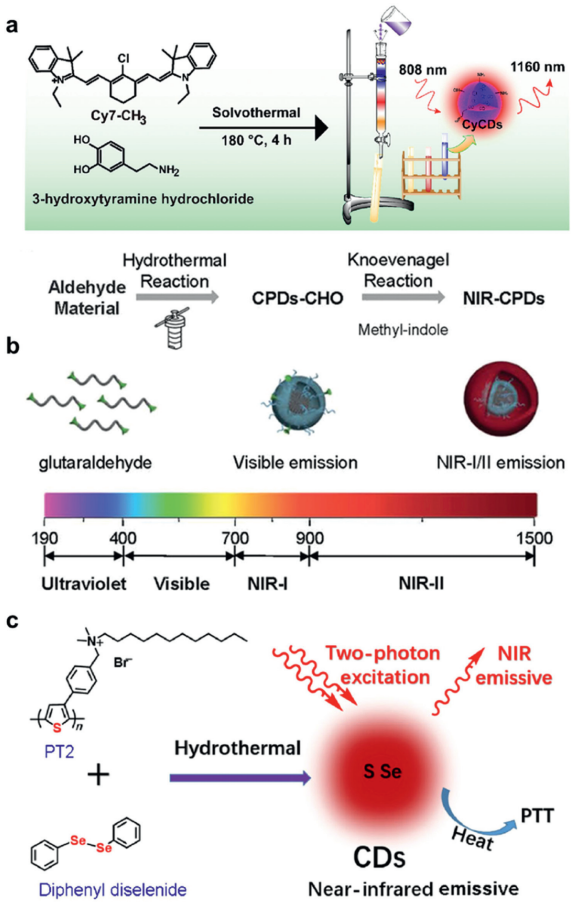

Fig. 4. (a) Schematic diagram of the synthesis of NIR CyCDs. Reproduced with permission [47]. Copyright 2023, Elsevier. (b) Schematic synthesis process of NIR-CPDs. Reproduced with permission [54]. Copyright 2022, The authors. (c) Schematic diagram of the preparation of polythiophene–derived NIR CDs. Reproduced with permission [56]. Copyright 2017, Springer Nature.

Among them, rare earth elements have intrinsic NIR emission, and when they are doped into CDs, CDs often inherit NIR emission [70–74]. For example, Wu *et al.* reported the synthesis of lanthanide hybrid carbon quantum dots (Ln-CQDs) through a simple one-pot hydrothermal method using citric acid as the carbon precursor and Yb^{3+} or Nd^{3+} as the doping ions. NIR emission peaks of Ln-CQDs are concentrated at about 998 nm and 1068 nm, respectively [71]. Naumov *et al.* reported that Nd- and Tm-doped CDs (Nd-GQDs/Tm-GQDs) have maximum emission at 1060 and 925 nm, respectively (Fig. S3a in Supporting information) [72].

Doping with other metal elements can also play a role. Yang *et al.* reported Ni and N co-doped CDs (Ni-CDs) for imaging-guided PTT in the NIR-II window (Fig. S3b in Supporting information). Ni-CDs exhibit significant absorption in the NIR-II region, with a PCE as high as 76.1% (1064 nm excitation) [61]. Wang *et al.* developed iron-doped CDs (Fe-CDs), which have an absorption peak at 830 nm and an emission peak at ~1000 nm in acidic solutions with a PLQY ~1.27%, can be used as an effective probe for *in vivo* NIR-II bioimaging [62]. Ge *et al.* used manganese phthalocyanine (II) as the raw material to synthesize Mn-doped CDs (Mn-CDs). Its NIR emission peak is located at 745 nm [50].

2.5.2. Non-metal element doping

Since most raw materials contain nitrogen sources, N is the most widely used dopant. Xiong *et al.* reported that as the nitrogen content and size of graphite gradually increase, the luminescence of CDs shifts gradually from blue to NIR [27]. Wang *et al.* reported that B, N co-doped CDs have a weak absorption broad peak at ~780 nm and an emission peak around 1000 nm under excitation by an 808 nm laser. The PLQY in the NIR region is about 1.0% (Fig. S3c in Supporting information) [66]. Jiang *et al.* reported that ammonium fluoride (NH_4F) was added as a dopant to the citric acid and urea system to obtain N, F co-doped CDs (N-CDs-F), which exhibited a NIR emission band at 777 nm with a PLQY of 9.8% in DMF [63]. Qu's group reported that nitrogen-doped NIR CDs were prepared by reacting large conjugated raw materials with urea. After surface passivation, the PLQY in the aqueous solution reached 8.3%, while in DMF it was as high as 18.8% [31].

It is worth noting that the above luminescence mechanisms do not always act alone, but more often act synergistically to lead to the NIR emission of CDs. The absorption peaks, NIR emission peaks, PLQY, and tested solvents of NIR CDs are summarized in Table S1 (Supporting information).

3. Applications of NIR CDs

NIR CDs have the advantages of low cytotoxicity, high biocompatibility, easy modification, deep penetration, little tissue damage, and low autofluorescence. Their applications are mainly concentrated in the biomedical field, such as NIR imaging, photoacoustic imaging, photothermal therapy (PTT), photodynamic therapy (PDT), PCT, and drug delivery. There are also some examples of NIR CDs applied in lasers, LEDs, and afterglow encryption.

3.1. Application of NIR CDs in bioimaging

3.1.1. NIR FLI and afterglow imaging

Biological fluids are aqueous environments, and CDs with efficient NIR fluorescence or afterglow in aqueous solutions are ideal reagents for biological imaging [29,31,33,37,56,62,66,75–78]. Qu's group developed large conjugated molecules of derived NIR luminescent CDs with a dominant absorption peak at 726 nm and dominant emission peak at 751 nm in aqueous solution and high PLQY (8.3% in aqueous solution, 18.8% in DMF), which was successfully used in NIR imaging of mouse intestinal and two-photon NIR imaging of mouse ear blood vessels (Figs. 5a and b) [31]. Ci *et al.* reported Fe-doped CDs (Fe-CDs) whose fluorescence emission showed a good linear relationship with pH in the wavelength range of 900–1200 nm and had a quantum yield of 1.27%. The Fe-CDs probe non-invasively monitors gastric pH changes during digestion in mice, suggesting its potential application in assisting imaging-guided diagnosis or therapeutic delivery of gastric diseases [62].

NIR afterglow bioimaging has the advantage of no background signal because the luminescence signal is collected only after the excitation light source stops [79]. Recently, Shan *et al.* developed a photooxidation-induced strategy to construct NIR afterglow luminescent CDs (afterglow peaks at 670 and 720 nm). The afterglow luminescence lifetime can reach 5.9 h, which is comparable to rare earth or organic long afterglow luminescent materials. At the same time, the CDs have a high imaging signal-to-noise ratio, good biosafety, and tumor-specific targeting ability. Based on this, the afterglow navigation technology was successfully applied to the precise resection of mouse tumor tissue, demonstrating its potential clinical application value (Fig. 5c). This work provides new research ideas for the development of afterglow luminescent materials suitable for the field of biological imaging [78].

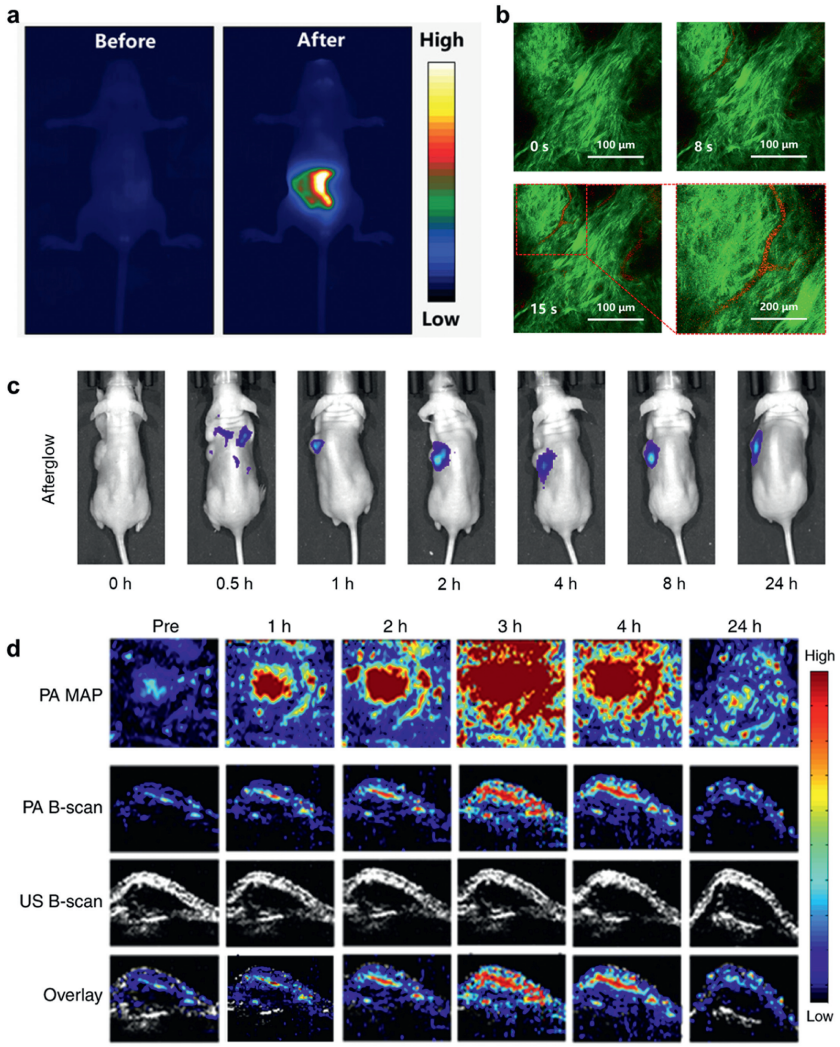

Fig. 5. (a) NIR CDs for single-photon NIR imaging of mouse intestine (Ex. 690 nm) and (b) two-photon angiography of mouse ear vessels (Ex. 1300 nm femtosecond pulse laser). Reproduced with permission [31]. Copyright 2022, The Authors. (c) Afterglow imaging in mouse tumor models. Reproduced with permission [78]. Copyright 2024, The Authors. (d) PA MAP images and B-scan PA images of the tumor. Reproduced with permission [81]. Copyright 2017, The Authors.

3.1.2. Photoacoustic imaging (PAI)

PAI is an emerging technology that has higher *in vivo* spatial resolution than FLI. Because tissue scatters acoustic signals much less than optical signals, PAI also has a deeper tissue penetration level for *in vivo* imaging. In PAI, contrast agents must possess a high molar extinction coefficient, absorb light within the NIR band, exhibit exceptional photothermal conversion efficiency, maintain high photostability, and demonstrate minimal toxicity levels [80]. CDs with efficient NIR light absorption and photothermal conversion properties are often excellent photoacoustic reagents. Under the irradiation of NIR light, the tissue where CDs are enriched is heated, and the thermoelastic expansion of biomolecules can generate acoustic waves that can be detected by PA imaging [81].

Qu's group reported the development of a new type of S, N-doped CDs from citric acid and urea *via* the solvothermal method in DMSO, which has a NIR emission peak at 720 nm and high photothermal conversion efficiency (59.2%) in aqueous CDs solution. After intravenous injection, CDs accumulated in tumor tissue and showed strong NIR fluorescence and PA signals *in vivo* (Fig. 5d). The maximum amplitude projection images and B-scan images of 4T1 tumors obtained at different time intervals post-injection vividly illustrated the homogeneous accumulation of CDs within the tumor tissue. These CDs emitted notably contrasted PA signals through blood circulation, with peak intensity observed at the 3-h mark post-injection [81].

3.2. Application of NIR CDs in diagnosis and therapy

3.2.1. PTT

Photoluminescence and photothermal conversion are competing processes. The former originates from the release of photons by radiative transitions of excited states, while the latter is a non-radiative transition, usually released in the form of thermal energy. NIR CDs with photothermal conversion effects often have very low PLQY of NIR luminescence or do not emit NIR luminescence. PTT is a treatment method that uses photothermal conversion materials to convert absorbed light energy into local heat to kill tumor cells. It has the advantages of accurate positioning, non-invasiveness, strong selectivity, minimal invasiveness, and good controllability, and can be combined with other treatment methods, making it a potentially important application prospect in tumor treatment [61,82]. NIR CDs with photothermal conversion effects are ideal reagents for PTT [33,39,40,56,61,66,81,83,84].

In 2017, Lan *et al.* reported that S and Se co-doped NIR emitting CDs have a PCE of 58.2% under 635 nm laser and can be used

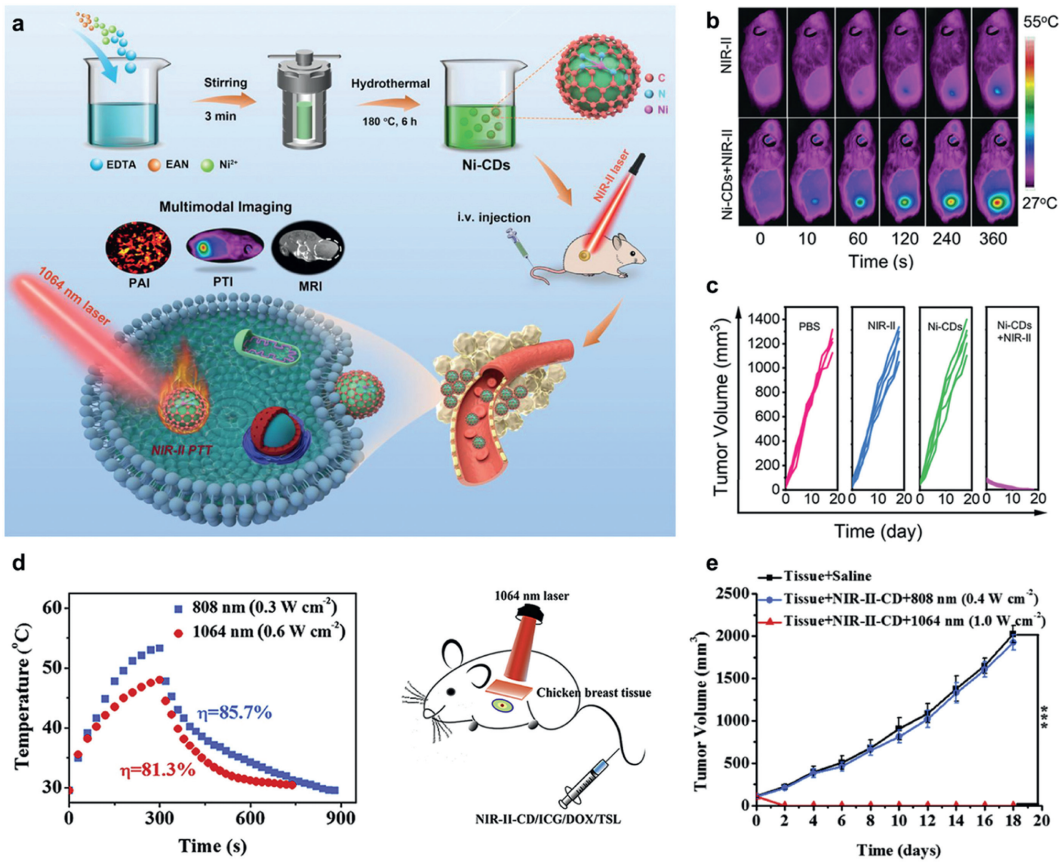

Fig. 6. (a) Schematic diagram of Ni-CDs used for NIR-II PTT of tumor. (b) Infrared thermal images at the tumor sites under 1064 nm irradiation (0.5 W/cm^2). (c) Change of tumor volumes after different treatments. Reproduced with permission [61]. Copyright 2021, John Wiley and Sons. (d) Photothermal effect of NIR-II-CDs sample under 1064 nm laser at 0.6 W/cm^2 and 808 nm at 0.3 W/cm^2 (left) and schematic diagram of NIR-II-CDs for tumor treatment (right). (e) Tumor growth curves of mice after intratumoral injection of NIR-II-CDs or saline with and without irradiation with 808 or 1064 nm laser. Reproduced with permission [40]. Copyright 2020, Elsevier.

for the PTT of tumor cells *in vitro* or *in vivo* [56]. In 2018, Qu's group reported that metal-free doped CDs simultaneously achieved NIR emission with a peak at 720 nm and high PCE (59.19%) under 655 nm laser irradiation. The CDs accumulated in tumor tissues after intravenous injection, and the tumors of mice treated with PTT were eradicated and the mice survived for more than three months without tumor recurrence [81]. The Ni-doped CDs (Ni-CDs) reported by Tian *et al.* have a high PCE of 76.1% under NIR second region (1064 nm) irradiation and can be effectively concentrated in the tumor site after tail vein injection. Even at a lower power density (0.5 W/cm^2), Ni-CDs exhibited satisfactory photothermal anti-tumor efficacy under 1064 nm laser irradiation (Figs. 6a-c) [61].

Geng *et al.* used 1,3,6-trinitropyrene and BPEI as raw materials and prepared NIR-absorbing CDs with controllable graphite N content by changing the precursor mass ratio. They found that the absorbance at 808 nm and 1064 nm was proportional to the graphite N content and the PEC increased significantly with the increase of graphite N content. Under 1064 nm laser irradiation, NIR-II-CDs had an ultra-high PCE of 81.3% [40]. Using NIR-II-CDs or their mixed liposome formulations as single PTT or image-guided PCT agents, the tumor was ablation without recurrence under 1064 nm NIR-II laser irradiation (Figs. 6d and e). Subsequently, Geng *et al.* formed hybrid materials or heterojunctions (HJs) with various materials with high PCEs using the CDs prepared by this method and obtained relatively high PCEs (56%–77%) [30,42,43], as detailed in Section 1.2.3 and Table S2 (Supporting information).

3.2.2. PDT/PCT

PDT is a non-invasive method for cancer treatment. Appropriate light activates photosensitizers (PS) to produce toxic reactive oxygen species (ROS) to oxidatively damage cancer cells [85,86]. An ideal PS should have the advantages of tumor targeting, low dark field toxicity, NIR light activation, and efficient ROS generation. Under NIR light irradiation, PS can undergo type I (electron transfer) reactions to produce toxic free radicals (peroxides, superoxide anions, hydroxyl radicals, *etc.*) or type II (energy transfer) photochemical reactions to produce singlet oxygen ($^1O_2$). Most PS reported so far are based on O_2-dependent type II pathways, where energy is transferred from the excited triplet state (T_1) of PS to O_2 by producing $^1O_2$. Compared with type II PDT, the excited type I PSs transfer electrons to the surrounding substrate or O_2 to produce $^{\bullet}O_2^-$, H_2O_2, and hydroxyl radicals ($^{\bullet}OH$), *etc.*, showing low O_2-dependent properties [87].

To obtain a NIR responsive PS, Ge *et al.* assembled CDs synthesized from polythiophene derivatives into nanospheres, which show a red-shifted absorption band and a NIR emission peak at 731 nm and can be excited by a 671 nm laser to produce $^1O_2$, the yield is about 0.45 (Table S3 in Supporting information). These CDs nanospheres can accumulate at the tumor site through enhanced permeability and retention effects, and completely inhibit the growth of tumors through PDT [58]. However, the hypoxia exhibited in larger tumors significantly weakens the anticancer effect. To overcome the hypoxic tumor microenvironment and prevent the rapid consumption of oxygen in PDT, the research group further synthesized Mn-doped CDs and assembled them with the help of

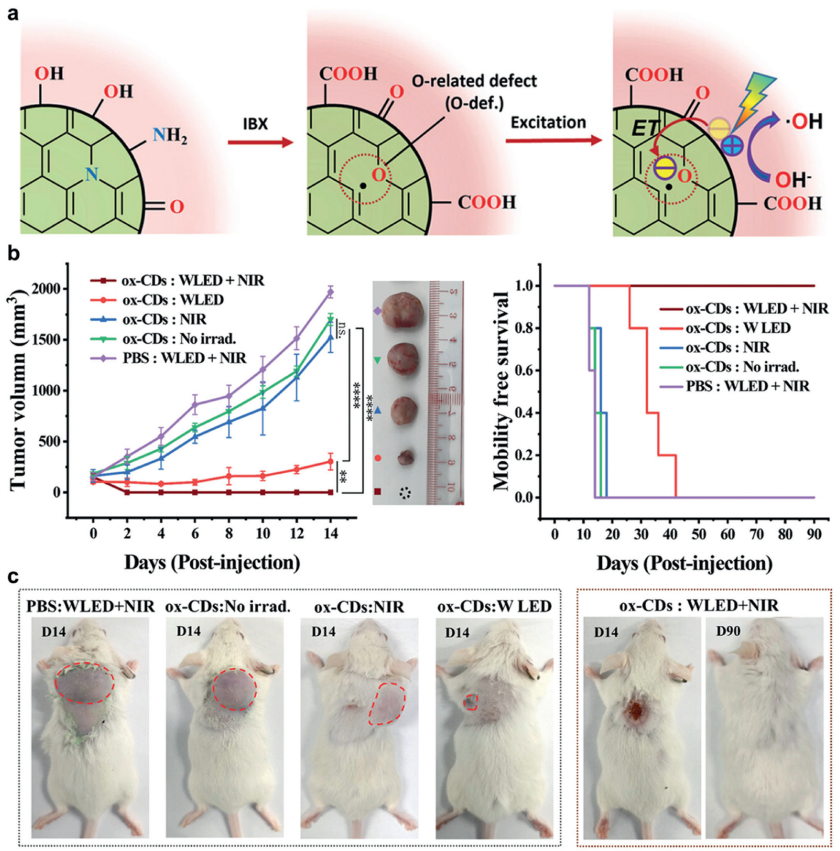

Fig. 7. (a) Schematic diagram of ox-CDs used in PCT. (b) Tumor growth curves of 4T1 tumors and representative tumors of mice after different treatments (left) and survival rates of G1–G5 mice (right). Photographs of G1–G5 mice on day 14 and G5 mice on day 90 (left). Reproduced with permission [29]. Copyright 2023, John Wiley and Sons.

liposomes, which can produce $^1O_2$ with a QY of 0.4. The Mn-CDs assembly can highly catalyze the production of oxygen from H_2O_2 and successfully improve tumor hypoxia, thereby improving PDT efficiency [50].

•OH has the highest oxidizing ability than other ROS and can cause more significant lipid peroxidation and oxidative DNA damage. Compared with PDT, the advantage of PCT is that it directly oxidizes water molecules to generate •OH with strong oxidizing ability, and does not depend on the concentration of dissolved oxygen or hydrogen peroxide in the tumor microenvironment [88]. Qu's group reported that NIR emitting CDs (ox-CDs) prepared by a post-oxidation process to construct oxygen-related defects strategy can catalyze the production of ·OH under the irradiation of 730 nm and white light LEDs, and are applied to the PTT-promoted PDT/PCT (Figs. 7a-c) [29]. The tumors in the combined white light LED flashlight and 730 nm laser irradiation group (G5) disappeared completely, and there was no recurrence after 90 days. A recent systematic review on the application of photo-responsive CDs in PDT/PCT is available for reference [89].

3.2.3. Sonodynamic therapy (SDT)

SDT is an innovative non-invasive treatment method that utilizes ultrasound technology. Ultrasound can penetrate tissues safely without significant attenuation, activating sonosensitizers to generate reactive oxygen species capable of killing tumor cells. Compared to PDT, SDT effectively addresses the challenge of light penetration in deep tumors. Recent studies have identified NIR CDs as promising sonosensitizers for SDT. Shen *et al.* developed NIR phosphorescent CDs using NIR dye ICG in combination with branched polyethyleneimine as raw materials, endowing them with effective SDT properties. When these CDs are loaded with cancer cell membranes, they can precisely target tumors, enhancing the efficacy of tumor-specific SDT [52]. Furthermore, when NIR CDs are covalently combined with gelatin methacrylamide (GelMA) to form hydrogels, the resulting NIR-CD/GelMA composite shows potential for bone repair in a mouse model of bone defect infection [90].

3.2.4. Synergy therapy

Compared with single-mode therapy, synergistic therapy can greatly improve the therapeutic effect of tumors. CDs can achieve synergistic therapy when used as imaging agents and photosensitizers or in combination with other photosensitizers, immune activators, and anticancer drugs. Zhou *et al.* synthesized NIR emitting CDs (emission peaks at 700 nm) of simulated amino acids with multiple pairs of edge α-carboxyl and amino-functionalized surfaces. The CDs with high tumor specificity *in vivo* can perform NIR FLI and PAI-guided delivery of chemotherapeutics to tumors in a targeted manner. CDs are loaded with the aromatic chemotherapy drug topotecan hydrochloride (TPTC) through π-π stacking interactions, which can even penetrate the blood-brain barrier and deliver TPTC to brain tumors [77].

Lin *et al.* reported heterojunction materials (CSCs@PEG) prepared from CDs and Co_9S_8, which had a PCE of 51.5% under 1064 nm excitation and led to the generation of ROS. CSCs@PEG exhibited GOx-like activity, which could not only reduce the energy supply in cells but also increase the H_2O_2 content. In addition, they also exhibited peroxidase, catalase, and GSH oxidase mimetic activities. Tandem multi-nanozyme activity can introduce starvation therapy and enhance chemotherapy (CDT) and PDT. Synergistic therapy (PTT/PDT/CDT) can also effectively stimulate the immune response, thereby achieving the goal of anti-cancer (Fig. 8) [60]. Shan *et al.* developed carbon nanogels (CNG) that possess

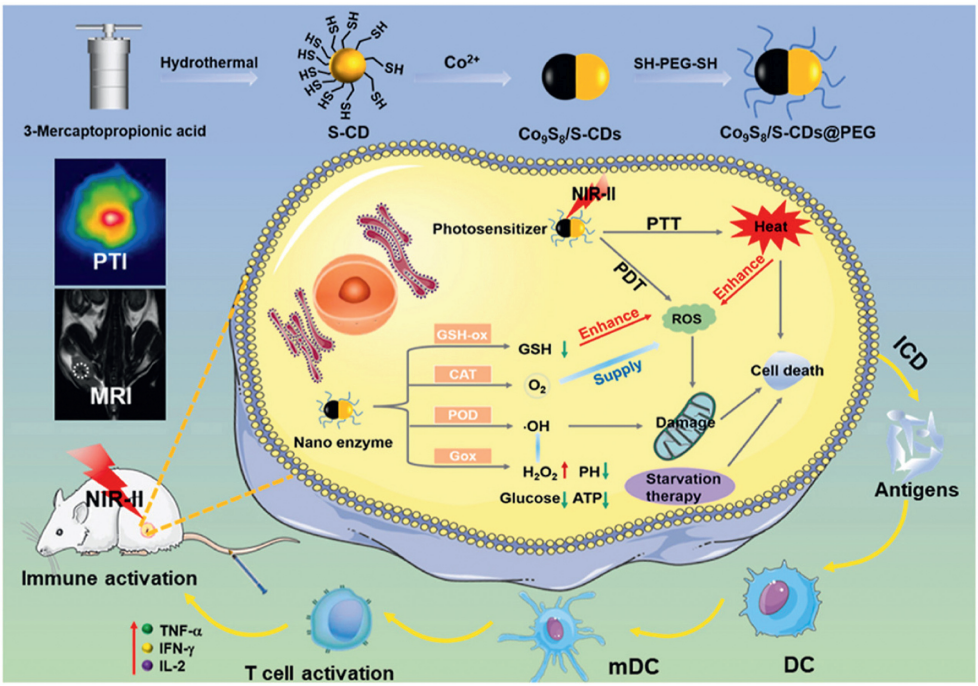

Fig. 8. Schematic diagram of CSCs@PEG material used as multifunctional anticancer synergistic therapy. Reproduced with permission [60]. Copyright 2022, Elsevier.

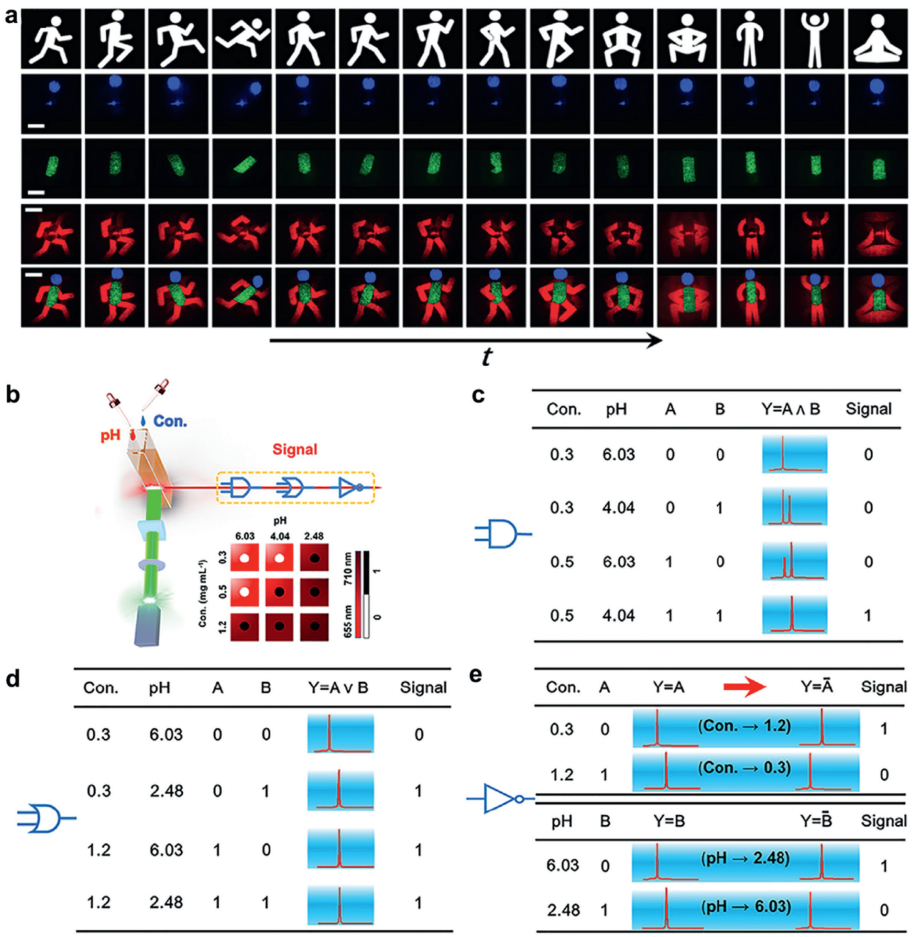

Fig. 9. (a) Speckle-free full-color laser imaging and colorful holographic displays based on CD lasers. Reproduced with permission [92]. Copyright 2023, John Wiley and Sons. (b) Schematic of the laser logic gate. Truth table for operation of logic gates including (c) AND, (d) OR, and (e) NOT operations. Reproduced with permission [93]. Copyright 2024, Elsevier.

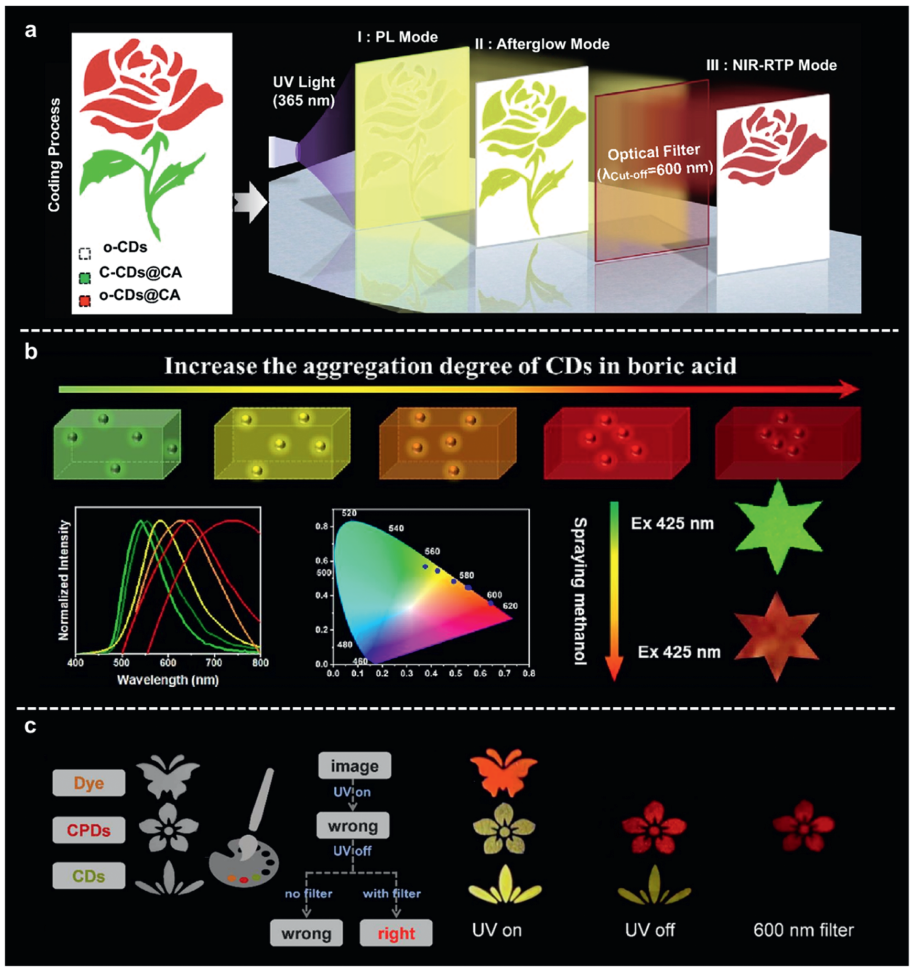

Fig. 10. (a) Schematic illustration of the encryption and decryption procedure using the *o*-CDs@CA in information security applications. Reproduced with permission [97]. Copyright 2021, The authors. (b) Phosphorescence spectra of visible to NIR phosphorescent CDs and their encryption applications. Reproduced with permission [98]. Copyright 2023, Elsevier. (c) Schematic illustration of the anti-counterfeiting of CPDs and photographs of patterns taken under different conditions. Reproduced with permission [100]. Copyright 2024, John Wiley and Sons.

dual functions for ROS imaging and performing PDT, utilizing self-assembled chemiluminescent (CL) conjugated CPDs. This innovative platform can be employed for *in vitro* and *in vivo* ROS bioimaging in animal inflammation models and demonstrates outstanding efficacy in the treatment of xenograft tumors [91].

3.3. Application of NIR CDs in luminescence

3.3.1. Lasers

NIR lasers have broad application prospects in space optical communications, lidar, *etc*., and the development of high-performance NIR CDs-based lasers is of great significance. However, there are a few examples of the report and application of NIR CDs in lasers. In 2023, Lu's research group reported bright blue to NIR fluorescence (714 nm) of CDs and placed them in the quartz cuvette respectively to achieve laser emission ranging from 467.3 nm to 705.1 nm, spanning 238 nm. Finally, using these CDs-based lasers as light sources, they successfully achieved color speckle-free laser imaging and dynamic high-quality holographic display (Fig. 9a) [92]. Recently, they achieved reversibly switchable dual-wavelength laser emission in the red and NIR using CDs derived from *o*-phenylenediamine [93]. The NIR-CDs can be fine-tuned by concentration or pH adjustment. At low concentrations or weak acid conditions, the main emission peak wavelength is 655 nm, while at high concentrations or strong acid conditions, it shifts to 710 nm. Simultaneous emission at 655 nm and 710 nm can be achieved by selecting moderate concentrations or moderate acid conditions. By leveraging the adaptable dual-wavelength laser capabilities of NIR-CDs, they successfully performed logic gate operations such as AND, OR, and NOT (Figs. 9b-e).

3.3.2. Light-emitting diodes

Plants need to absorb blue, red, and NIR light for photosynthesis. NIR high-efficiency luminescent CDs can be used with blue LED chips to prepare plant growth lighting LEDs. Also, NIR luminescent CDs can be used with luminescent materials in other bands of visible light to prepare white LEDs. Xiong *et al*. prepared full-color luminescent CDs, using blue CDs (B-CDs), green CDs (G-CDs), and NIR CDs (R-CDs, emission peak at 715 nm). When mixed and dispersed in the polyvinyl alcohol (PVA) matrix, a pure white light-emitting CDs/PVA composite film with CIE color coordinates (0.33, 0.33) is obtained, and the PLQY is as high as 39% [27]. Recently, Wang *et al*. prepared solid-state fluorescent emitting CDs from the visible to NIR region (540–720 nm). Using these CDs as conversion phosphors, white LEDs with tunable correlated color temperatures of 1882–5019 K can be manufactured. Plant-growth LED devices were prepared using blue LED chips and deep red/NIR emitting CDs. Compared with sunlight and white light LEDs, peanuts illuminated by plant growth LEDs show higher growth efficiency in biomass [35].

In addition to photoluminescent LEDs, electroluminescent LEDs represent another significant luminescent application. Yuan *et al.* utilized natural green plants as carbon sources to synthesize CDs exhibiting deep red to NIR narrow bandwidth emission through a solvothermal method, with emission peaks at 673 nm and 720 nm. The resulting electroluminescent device demonstrated deep red to NIR emission, with International Commission on Illumination (CIE) coordinates of (0.692, 0.307). The maximum brightness (L_{max}) of the CD-LED surpassed 500 cd/m², paving the way for low-cost, environmentally friendly CDs suitable for high-color purity displays and specialized lighting applications [94]. A recent review on the electroluminescence of CDs is available for reference [95].

3.3.3. Afterglow encryption

CDs confined in external matrices such as boric acid (BA), polymers, zeolite, or CDs with self-confined structures can emit phosphorescence [96]. This is because the rigid structure restricts the non-radiative dissipation of CDs such as vibration and rotation, promoting the occurrence of intersystem crossing (ISC) and the generation of triplet excitons. CDs showing afterglow properties show unique talents in information encryption/anti-counterfeiting [97–99]. Wang *et al.* reported a simple method to achieve green thermally activated delayed fluorescence (TADF) and NIR room temperature phosphorescence (RTP) in the composites of *o*-CDs and cyanuric acid (Fig. 10a) [97]. Qu's group increased the content of CDs in BA during the heat treatment process, and the degree of aggregation of CDs gradually increased, causing a large number of electron interactions, which in turn led to energy splitting and the formation of low-energy aggregation states, which led to phosphorescence from 530 nm to 750 nm. The solvent-triggered evolutionary discoloration properties of CDs were further developed and applied in advanced anti-counterfeiting and information encryption (Fig. 10b) [98]. Recently, Yang's group developed self-protective CPDs with NIR RTP (710 nm). The RTP emission is promoted by the generation of triplet excitons protected by the cross-linked network inside the nanoparticles [100]. The CPDs with NIR RTP emission exhibit great potential in multi-mode information encryption, and multi-mode anti-counterfeiting (Fig. 10c).

4. Summary and outlook

This review systematically reviews the development of CDs with absorption and emission in the NIR band (≥700 nm) and summarizes in detail the reported preparation strategies of NIR CDs and their applications in NIR bioimaging, NIR light responsive phototherapy (PTT, PDT, PCT, synergy therapy), as well as their application in NIR luminescence (lasers, LEDs and afterglow information encryption). Overall, the research on NIR absorbing/luminescent CDs is still in its early stages, and there is a lot of room for future development.

Although the research on NIR CDs has made some progress, there are still the following problems to be solved:

(1) The controllable synthesis mechanism of NIR CDs is still unclear. The current reports on NIR CDs are mostly a few successful examples obtained through a large number of experiments, and the general synthesis strategies are still relatively vague. The purification standards of NIR CDs are not uniform and there are still problems with repeatability.
(2) The wavelength region of the incident light inevitably affects the penetration depth and resolution of PAI. At the same time, the PCE of the photoacoustic contrast agent will affect the temperature of the target tissue and the intensity of the generated sound waves. Therefore, it is necessary to further develop CDs with NIR long-wavelength absorption, high photothermal conversion efficiency, and tumor tissue targeting to achieve efficient PAI and PTT synergistic treatment.
(3) At present, the emission wavelength of NIR CDs is generally short, and there is a lack of reports on CDs with emission in the NIR-II region (1000–1700 nm). Photons in the NIR-II window have longer wavelengths, are less scattered in biological tissues, and have a longer attenuation length when propagating in biological tissues, which is beneficial for deep biological detection.
(4) Biological fluids are in a water environment, and there are few examples of high PLQY and stability in aqueous solutions, which limits the biological application of NIR CDs.
(5) There are only a few examples of CDs that emit NIR afterglow in aqueous solution. Phosphorescent bioimaging has great potential due to its lack of background noise, and it is imperative to develop more aqueous NIR phosphorescent CDs.
(6) Developing more NIR-induced PDT/PCT CDs that can generate type I reactive oxygen species can broaden their application in tumor treatment.
(7) The development of NIR afterglow CDs is essential for advanced information encryption applications. While utilizing external solid-state substrates presents a feasible solution, it can hinder applications in paper printing. Therefore, the future trend is to focus on the development of CDs with self-protective structures.

The above summary provides unique but limited insights into the formation mechanism, optical characteristics, applications, *etc.* of NIR CDs. It is believed that with further in-depth research, the synthesis strategy and luminescence mechanism of NIR CDs will become increasingly clear, their application scope will become wider and wider, and will make extraordinary contributions to solving current challenges.

Declaration of competing interest

The authors declare that they have no known competing financial interests or personal relationships that could have appeared to influence the work reported in this paper.

CRediT authorship contribution statement

Yupeng Liu: Writing – review & editing, Writing – original draft, Conceptualization. **Hui Wang:** Investigation, Methodology. **Songnan Qu:** Writing – review & editing, Supervision, Project administration, Funding acquisition, Conceptualization.

Acknowledgment

This work was financially supported by the Science and Technology Development Fund of Macau SAR (Nos. 0139/2022/A3, 0007/2021/AKP, 006/2022/ALC).

Supplementary materials

Supplementary material associated with this article can be found, in the online version, at doi:10.1016/j.cclet.2024.110618.

References

[1] C. Li, G. Chen, Y. Zhang, et al., J. Am. Chem. Soc. 142 (2020) 14789–14804.
[2] Y. Chen, S. Wang, F. Zhang, Nat. Rev. Bioeng. 1 (2023) 60–78.
[3] G. Hong, A.L. Antaris, H. Dai, Nat. Biomed. Eng. 1 (2017) 0010.
[4] K. Welsher, Z. Liu, S.P. Sherlock, et al., Nat. Nanotechnol. 4 (2009) 773–780.
[5] G. Hong, J.T. Robinson, Y. Zhang, et al., Angew. Chem. Int. Ed. 51 (2012) 9818–9821.
[6] A.L. Antaris, H. Chen, K. Cheng, et al., Nat. Mater. 15 (2016) 235–242.
[7] R.X. Wang, Y. Ou, Y. Chen, et al., J. Am. Chem. Soc. 146 (2024) 11669–11678.
[8] L. Đorđević, F. Arcudi, M. Cacioppo, M. Prato, Nat. Nanotechnol. 17 (2022) 112–130.
[9] Y.P. Sun, B. Zhou, Y. Lin, et al., J. Am. Chem. Soc. 128 (2006) 7756–7757.

[10] X. Xu, R. Ray, Y. Gu, et al., J. Am. Chem. Soc. 126 (2004) 12736–12737.
[11] Y. Hu, O. Seivert, Y. Tang, et al., Angew. Chem. Int. Ed. 63 (2024) e202412341.
[12] H. Xu, J. Chang, H. Wu, et al., Small 19 (2023) 2207204.
[13] W. Su, H. Wu, H. Xu, et al., Mat. Chem. Front. 4 (2020) 821–836.
[14] T. Yuan, F. Yuan, L. Sui, et al., Angew. Chem. Int. Ed. 62 (2023) e202218568.
[15] D. Pan, J. Zhang, Z. Li, M. Wu, Adv. Mater. 22 (2010) 734–738.
[16] X. Niu, W. Zheng, T. Song, et al., Chin. Chem. Lett. 34 (2023) 107560.
[17] X. Niu, T. Song, H. Xiong, Chin. Chem. Lett. 32 (2021) 1953–1956.
[18] H. Ding, R. Zhao, Z.H. Zhang, et al., Chem. Eng. J. 476 (2023) 146405.
[19] W.J. Zheng, Z.N. Sun, Y.M. Wang, H.M. Xiong, Nano Res. 17 (2024) 8495–8503.
[20] K. Jiang, S. Sun, L. Zhang, et al., Angew. Chem. Int. Ed. 54 (2015) 5360–5363.
[21] Z. Tian, X. Zhang, D. Li, et al., Adv. Opt. Mater. 5 (2017) 1700416.
[22] Y. Liu, J. Yang, Y. Hao, S. Qu, Chem. J. Chin. Univ. (2024), doi:10.7503/cjcu20240070.
[23] H. Ding, X.X. Zhou, J.S. Wei, et al., Carbon 167 (2020) 322–344.
[24] A. Lv, Q. Chen, C. Zhao, et al., Chin. Chem. Lett. 32 (2021) 3653–3664.
[25] Y. Jiang, T. Zhao, W. Xu, Z. Peng, Carbon 219 (2024) 118838.
[26] W. Qin, M. Wang, Y. Li, et al., Mat. Chem. Front. 8 (2024) 930–955.
[27] H. Ding, J.S. Wei, P. Zhang, et al., Small 14 (2018) 1800612.
[28] D. Li, C. Liang, E.V. Ushakova, et al., Small 15 (2019) 1905050.
[29] T. Zhang, Q. Cheng, J.H. Lei, et al., Adv. Mater. 35 (2023) 2302705.
[30] B. Geng, H. Qin, W. Shen, et al., Chem. Eng. J. 383 (2020) 123102.
[31] Y. Liu, J.H. Lei, G. Wang, et al., Adv. Sci. 9 (2022) 2202283.
[32] D. Li, P. Jing, L. Sun, et al., Adv. Mater. 30 (2018) 1705913.
[33] M. Zheng, Y. Li, S. Liu, et al., ACS Appl. Mater. Interfaces 8 (2016) 23533–23541.
[34] M.A. Sk, A. Ananthanarayanan, L. Huang, et al., J. Mater. Chem. C 2 (2014) 6954–6960.
[35] B. Xu, J. Li, J. Zhang, et al., Adv. Sci. 10 (2023) 2205788.
[36] Y. Hu, C. Neumann, L. Scholtz, et al., Nano Res. 16 (2023) 45–52.
[37] S. Lu, L. Sui, J. Liu, et al., Adv. Mater. 29 (2017) 1603443.
[38] S. Qu, D. Zhou, D. Li, et al., Adv. Mater. 28 (2016) 3516–3521.
[39] D. Li, D. Han, S.N. Qu, et al., Light Sci. Appl. 5 (2016) e16120–e16120.
[40] B. Geng, W. Shen, F. Fang, et al., Carbon 162 (2020) 220–233.
[41] B. Geng, W. Shen, P. Li, et al., ACS Appl. Mater. Interfaces 11 (2019) 44949–44960.
[42] L. Yan, Z. Cao, L. Ren, et al., Adv. Healthc. Mater. 13 (2024) 2302190.
[43] B. Geng, L. Yan, Y. Zhu, et al., Adv. Healthc. Mater. 12 (2023) 2202154.
[44] C.F. Chiu, W.A. Saidi, V.E. Kagan, A. Star, J. Am. Chem. Soc. 139 (2017) 4859–4865.
[45] L. Fu, X. Gao, S. Dong, et al., Anal. Chem. 93 (2021) 4909–4915.
[46] M. Jain, Manju, A. Gundimeda, et al., Appl. Surf. Sci. 480 (2019) 945–950.
[47] W. Liu, B. Wu, W. Sun, et al., Chem. Eng. J. 471 (2023) 144530.
[48] E.A. Stepanidenko, I.D. Skurlov, P.D. Khavlyuk, et al., Nanomaterials 12 (2022) 543.
[49] D. Jana, D. Wang, P. Rajendran, et al., JACS Au 1 (2021) 2328–2338.
[50] Q. Jia, J. Ge, W. Liu, et al., Adv. Mater. 30 (2018) 1706090.
[51] W. Liu, H. Gu, W. Liu, et al., Chem. Eng. J. 450 (2022) 137384.
[52] B. Geng, J. Hu, Y. Li, et al., Nat. Commun. 13 (2022) 5735.
[53] Y. Jiang, Z. Tan, T. Zhao, et al., Nanoscale 15 (2023) 1925–1936.
[54] T. Han, Y. Wang, S. Ma, et al., Adv. Sci. 9 (2022) 2203474.
[55] D. Huang, H. Zhou, Y. Wu, et al., Carbon 142 (2019) 673–684.
[56] M. Lan, S. Zhao, Z. Zhang, et al., Nano Res. 10 (2017) 3113–3123.
[57] Y. Wang, X. Li, S. Zhao, et al., Coord. Chem. Rev. 470 (2022) 214703.
[58] Q. Jia, J. Ge, W. Liu, et al., Adv. Healthc. Mater. 6 (2017) 1601419.
[59] N. Wang, T. Dong, W. Shi, et al., J. Mater. Chem. B 11 (2023) 6372–6382.
[60] K. Kang, L. Wang, Y. Ma, et al., Carbon 197 (2022) 98–111.
[61] B. Tian, S. Liu, L. Feng, et al., Adv. Funct. Mater. 31 (2021) 2100549.
[62] Q. Ci, Y. Wang, B. Wu, et al., Adv. Sci. 10 (2023) 2206271.
[63] L. Jiang, H. Ding, M. Xu, et al., Small 16 (2020) 2000680.
[64] B. Wang, J. Yu, L. Sui, et al., Adv. Sci. 8 (2021) 2001453.
[65] S. Sarkar, K. Das, M. Ghosh, P.K. Das, RSC Adv. 5 (2015) 65913–65921.
[66] H. Wang, Q. Mu, K. Wang, et al., Appl. Mater. Today 14 (2019) 108–117.
[67] H. Ding, J. Xu, L. Jiang, et al., Chin. Chem. Lett. 32 (2021) 3646–3651.
[68] X. Li, Y. Fu, S. Zhao, et al., Chem. Eng. J. 430 (2022) 133101.
[69] H. Shi, Y. Yin, H. Xu, et al., Chem. Eng. J. 488 (2024) 150661.
[70] J. Liu, X. Ge, L. Sun, et al., RSC Adv. 6 (2016) 47427–47433.
[71] F. Wu, H. Su, X. Zhu, et al., J. Mater. Chem. B 4 (2016) 6366–6372.
[72] M.T. Hasan, R. Gonzalez-Rodriguez, C.W. Lin, et al., Adv. Opt. Mater. 8 (2020) 2000897.
[73] M. Zhang, X. Zhai, M. Sun, et al., Chem. Soc. Rev. 49 (2020) 9220–9248.
[74] Q. Zhu, L. Zhang, K. Van Vliet, et al., ACS Appl. Mater. Interfaces 10 (2018) 10409–10418.
[75] H. He, Z. Wang, T. Cheng, et al., ACS Appl. Mater. Interfaces 8 (2016) 28529–28537.
[76] D. Sar, F. Ostadhossein, P. Moitra, et al., Adv. Sci. 9 (2022) 2202414.
[77] S. Li, W. Su, H. Wu, et al., Nat. Biomed. Eng. 4 (2020) 704–716.
[78] G.S. Zheng, C.L. Shen, C.Y. Niu, et al., Nat. Commun. 15 (2024) 2365.
[79] Z. Li, Q. Pei, Y. Zheng, et al., Chem. Eng. J. 467 (2023) 143384.
[80] H.B. Cheng, Y. Li, B.Z. Tang, J. Yoon, Chem. Soc. Rev. 49 (2020) 21–31.
[81] X. Bao, Y. Yuan, J. Chen, et al., Light Sci. Appl. 7 (2018) 91.
[82] W.B. Zhao, D.D. Chen, K.K. Liu, et al., Chem. Eng. J. 452 (2023) 139231.
[83] B. Geng, D. Yang, D. Pan, et al., Carbon 134 (2018) 153–162.
[84] Y. Li, G. Bai, S. Zeng, J. Hao, ACS Appl. Mater. Interfaces 11 (2019) 4737–4744.
[85] H. Cai, X. Wu, L. Jiang, et al., Chin. Chem. Lett. 35 (2024) 108946.
[86] Y. Yang, H. Ding, Z. Li, et al., Molecules 27 (2022) 8627.
[87] Y. Zhang, Q. Jia, F. Nan, et al., Biomaterials 293 (2023) 121953.
[88] H. Zhang, Q. Cheng, J.H. Lei, et al., J. Colloid Interface Sci. 644 (2023) 107–115.
[89] H. Zhang, Y. Liu, S. Qu, Responsive Mater. 2 (2024) e20240012.
[90] J. Tang, J. Hu, X. Bai, et al., Small 20 (2024) 2404900.
[91] C. Shen, T. Jiang, Q. Lou, et al., SmartMat 3 (2022) 269–285.
[92] Y. Zhang, J. Wang, L. Wang, et al., Adv. Mater. 35 (2023) 2302536.
[93] Y. Zhang, S. Ding, J. Yu, et al., Matter 7 (2024) 3518–3536.
[94] R. Chen, Z. Wang, T. Pang, et al., Adv. Mater. 35 (2023) 2302275.
[95] Y. Shi, W. Su, F. Yuan, et al., Adv. Mater. 35 (2023) 2210699.
[96] Z. Song, Y. Shang, Q. Lou, et al., Adv. Mater. 35 (2023) 2207970.
[97] Y. Wang, K. Jiang, J. Du, et al., Nano-Micro Lett. 13 (2021) 198.
[98] Q. Li, D. Cheng, H. Gu, et al., Chem. Eng. J. 462 (2023) 142339.
[99] K. Wang, L. Qu, C. Yang, Small 19 (2023) 2206429.
[100] C. Zheng, S. Tao, X. Zhao, et al., Angew. Chem. Int. Ed. 63 (2024) e202408516.